FULL PAPER

Batteries

ADVANCED
ENERGY
MATERIALS

www.advenergymat.de

On the Capacity Losses Seen for Optimized Nano-Si Composite Electrodes in Li-Metal Half-Cells

Fredrik Lindgren, David Rehnlund,* Ruijun Pan, Jean Pettersson, Reza Younesi, Chao Xu, Torbjörn Gustafsson, Kristina Edström, and Leif Nyholm

While the use of silicon-based electrodes can increase the capacity of Li-ion batteries considerably, their application is associated with significant capacity losses. In this work, the influences of solid electrolyte interphase (SEI) formation, volume expansion, and lithium trapping are evaluated for two different electrochemical cycling schemes using lithium-metal half-cells containing silicon nanoparticle–based composite electrodes. Lithium trapping, caused by incomplete delithiation, is demonstrated to be the main reason for the capacity loss while SEI formation and dissolution affect the accumulated capacity loss due to a decreased coulombic efficiency. The capacity losses can be explained by the increasing lithium concentration in the electrode causing a decreasing lithiation potential and the lithiation cut-off limit being reached faster. A lithium-to-silicon atomic ratio of 3.28 is found for a silicon electrode after 650 cycles using 1200 mAhg^{-1} capacity limited cycling. The results further show that the lithiation step is the capacity-limiting step and that the capacity losses can be minimized by increasing the efficiency of the delithiation step via the inclusion of constant voltage delithiation steps. Lithium trapping due to incomplete delithiation consequently constitutes a very important capacity loss phenomenon for silicon composite electrodes.

Dr. F. Lindgren, Dr. D. Rehnlund, Dr. R. Pan, Dr. R. Younesi, Dr. C. Xu, Dr. T. Gustafsson, Prof. K. Edström, Prof. L. Nyholm
Department of Chemistry – The Ångström Laboratory
Uppsala University
Box 538, 75121 Uppsala, Sweden
E-mail: David.Rehnlund@kemi.uu.se

Dr. D. Rehnlund
Institute for Applied Biosciences
Department of Applied Biology
Karlsruhe Institute of Technology
Fritz-Haber-Weg 2, 76131 Karlsruhe, Germany

Dr. J. Pettersson
Department of Chemistry – BMC
Uppsala University
Box 599, 75121 Uppsala, Sweden

Dr. C. Xu
Department of Chemistry
University of Cambridge
Lensfield Road, Cambridge CB2 1EW, UK

1. Introduction

New electrode materials are required to meet the demand for Li-based batteries with better performances.[1] Among the new material candidates for negative electrodes, silicon is particularly interesting as it may provide about an order of magnitude higher gravimetric as well as volumetric energy densities compared to the graphite-based negative electrodes typically employed today.[2] However, the realization of commercial silicon electrodes is hampered by the presence of large irreversible capacities, electrolyte decomposition problems, and the significant capacity losses seen during their cycling.[3] The latter losses are generally ascribed to two effects, i.e., the formation of a solid electrolyte interphase (SEI) layer and the volume changes associated with the silicon lithiation and delithiation reactions.

The SEI formation stems from the fact that at the low potentials of most negative electrode materials, the electrolyte solvents undergo reduction until the electrode becomes passivated by an SEI layer.[4] In full cell batteries, where the capacity of the positive electrode is capacity limiting, the SEI formation gives rise to a decrease in the cell capacity due to the consumption of a part of the capacity of the positive electrode.[5] For Si electrodes, the integrity of the SEI layer is also affected by the significant volume variations taking place during the cycling as this may lead to exposure of new surfaces that also require passivation via SEI formation.[3] If new surfaces are constantly formed, or if some of the SEI components dissolve in the electrolyte,[6] the SEI formation becomes a continuous process draining the capacity of the full-cell battery.[7] The irreversible SEI formation also gives rise to decreased coulombic efficiencies. It is, however, important to note that the SEI formation does not affect the charge storage capacity of the negative electrode and that in a half-cell battery, equipped with a lithium-metal counter electrode, the huge capacity of the latter usually compensates for the charge associated with the SEI formation. The significant capacity losses typically seen for silicon electrodes upon cycling in lithium-metal half-cells, can therefore not be explained by SEI formation.

Volume changes, yielding cracked particles, and loss of electrical contact to the particles, can, on the other hand, give rise to capacity losses for silicon electrodes cycled in lithium-metal

ADVANCED
SCIENCE NEWS
www.advancedsciencenews.com

ADVANCED
ENERGY
MATERIALS
www.advenergymat.de

half-cells.[8] For silicon, the volume expansion upon full lithiation has been estimated to 280% assuming that Li$_{3.75}$Si is formed.[9] While it is well known that there can be significant losses of active material for micrometer-sized silicon particles,[10] the influence of the effect can be significantly decreased if nanometer-sized silicon particles and efficient binders are employed.[11,12]

As significant capacity losses are generally still seen even for electrodes composed of nanometer-sized silicon particles, it was recently proposed[6] that the capacity losses seen for silicon (and other alloy forming electrode materials such as tin and aluminum) instead mainly stem from diffusion controlled trapping of lithium in the electrodes. The latter stems from the inability to completely delithiate the electrode after the lithiation step due to the fact that a small fraction (i.e., less than 1%) of the deposited lithium continues to diffuse toward the inner part of the electrode even during the delithiation step. This two-way diffusion results in a gradual increase in the lithium concentration in the electrode, which can be readily seen by determining the lithium concentration in the electrode as a function of the cycle number using, e.g., inductive coupled plasma–atomic emission spectroscopy (ICP-AES). Although the Li-trapping hypothesis[6] is relatively new, trapped lithium in electrodes has in fact already been observed for silicon using neutron reflectometry[13] and considered by other groups in different ways (e.g., as incomplete delithiation and slow delithiation kinetics, etc.)[14] and also for intermetallic compounds.[15] A significant amount of Li$_{3.75}$Si was also observed in a delithiated silicon electrode employing ex situ nuclear magnetic resonance (NMR).[16] It should be noted that the amorphous nature of many Li–Si phases makes the detection of any lithium containing phases in the silicon electrodes challenging and that the lithium concentrations in the delithiated electrode materials are very low unless the electrode has been cycled for many cycles. While the trapped lithium often has been ascribed to the formation of irreversible phases and slow delithiation kinetics, the reasons for the latter effects have not been properly explained so far. Other researchers have instead proposed that the irreversibly lost lithium was located within the SEI layer.[17] Given that the experimental data support the presence of trapped lithium and the significant potential impact of this effect, it is clearly very important to study the lithium-trapping phenomenon further using different cycling conditions, electrolytes, and characterization techniques.

In our previous lithium-trapping study,[6] we found that incomplete delithiation could explain the capacity losses seen for lithium-metal half-cells comprising tin nanorod electrodes or silicon composite electrodes containing 50 nm sized Si particles. It was also shown that the capacity increased rather than decreased during the initial cycles where the most dramatic effects of the volume variations would be expected, and that SEI formation did not affect the charge storage capacity of the electrodes. The incomplete delithiation, due to the diffusion-controlled trapping of lithium in the electrode, decreased the coulombic efficiency as well as the charge storage capacity of the electrode material as further lithiation was found to become more difficult.[6] The underlying trapping mechanism was explained based on diffusion of lithium toward the inner parts of the electrode rendering a small fraction (less than 1%) of the deposited lithium inaccessible during the subsequent delithiation step.[6] The results, however, also indicated that the influence of the lithium-trapping effect depends on the time scale of the lithiation and delithiation steps, as well as the lithium diffusion length in the electrodes. While it was concluded that it should be possible to decrease the influence of the lithium-trapping effect by improving the efficiency of the delithiation step, this approach was not studied in detail. Moreover, it is still not immediately clear why increasing lithium concentrations in the silicon electrode give rise to the observed capacity decreases and why the delithiation of the almost fully lithiated electrode was unsuccessful even though the electrode clearly contained large amounts of lithium. Other important questions concern the influences of the time domains of the lithiation and delithiation steps and the possibilities of increasing the efficiency of the delithiation step by using alternative cycling protocols, e.g., involving capacity limited cycling or asymmetric cycling with lithiation and delithiation steps of different durations. As lithium trapping should not lead to irreversible losses of capacity, the possibility of regenerating the electrode clearly needs be studied further since such approaches can be expected to have considerable implications on the use of not only silicon electrodes but also alloy forming electrodes in general.

The aim of the present work is to address the abovementioned questions using capacity limited cycling of lithium-metal based half-cells comprising silicon nanoparticle–based composite electrodes and an electrolyte especially designed to provide well-functioning SEI layers. By monitoring the capacity and accumulated capacity loss (i.e., the sum of the differences between the lithiation and delithiation charges for all cycles) and calculating the charge associated with the amount of lithium found in a cycled silicon electrode using ICP-AES, it is demonstrated that the capacity loss mainly can be ascribed to lithium trapping. The charge associated with the SEI formation and the SEI dissolution rate are likewise estimated from the experimental data. More importantly, by using two different cycling protocols, i.e., conventional constant current (CC) and constant current cycling combined with an additional constant voltage (CCCV) delithiation step, it is clearly shown that the lifetime of silicon electrodes can be increased significantly merely by increasing the efficiency of the delithiation step. The increase in the lithium concentration in the electrode, which is also monitored using hard X-ray photoelectron spectroscopy (HAXPES) experiments, is demonstrated to cause a gradual saturation of the electrode yielding a decrease in the lithiation voltage and the lithium diffusion coefficient in the silicon electrode. The latter cause the lithiation cut-off voltage to be reached faster and faster and the capacity to decrease gradually during cycling. Asymmetric cycling including lithiation and delithiation steps with different durations is also investigated as a means of increasing the lifetime of the silicon electrodes. Finally, the fundamental features of the lithium trapping phenomenon and the influence of the cycling protocol on the electrochemical performance of silicon electrodes are discussed.

ADVANCED
SCIENCE NEWS
www.advancedsciencenews.com

ADVANCED
ENERGY
MATERIALS
www.advenergymat.de

2. Results and Discussion

2.1. Capacity Limited Cycling

In the present work, the electrolyte composition and the cycling conditions (see **Figure 1**) were chosen to optimize the lifetime of the silicon nanoparticle–based composite electrodes. As one common strategy to prolong the lifetime of silicon electrodes is to use capacity limited cycling,[3] the performances of the half-cells were evaluated using constant lithiation and delithiation at a fixed capacity of 1200 mAh g^{-1} (i.e., 1.2 mAh cm^{-2}). This capacity corresponds to about 33% of the theoretical capacity for silicon. The silicon electrode was assumed to be capacity limiting due to the lithium-metal counter electrode employed in the half-cell and the lithiation and delithiation cut-off limits were set to 0.01 and 1.0 V versus Li$^+$/Li, respectively. The cycling protocol, hence, included a primary coulombic limit and a secondary voltage limit, so that the lithiation step was stopped if the potential of the silicon electrode reached 0.01 V versus Li$^+$/Li. The delithiation step was analogously interrupted if the potential reached 1.0 V versus Li$^+$/Li. Figure 1 illustrates the performances of the silicon electrodes during

i) capacity limited cycling (i.e., constant current cycling, CC) and ii) capacity limited cycling with constant current lithiation and constant current, constant voltage (CCCV) delithiation. In the latter case, the delithiation was carried out with a constant current step followed by a voltage pulse to 1.0 V versus Li$^+$/Li on every 10th cycle. The only difference between the cycling protocols was hence the constant voltage delithiation step used in the CCCV case.

As seen in Figure 1A, the intended capacity limited cycling performance could be maintained for almost 300 cycles when using the standard (i.e., CC) cycling protocol. However, a dramatic capacity decline was observed after about 300 cycles with the capacity dropping from 1200 to a few mAh g^{-1} during only about 50 cycles. Prior to this, i.e., after about 280 cycles, a marked decrease could be seen in the coulombic efficiency (see Figure 1B) indicating a marked change in the electrochemical behavior. The coulombic efficiency (i.e., the ratio between the delithiation and lithiation capacities) was, incidentally, about 98% initially but was found to have increased to slightly above 99% after 100 cycles. As the lithium-metal counter electrode should have been be able to compensate for SEI formation charge, the observed capacity decrease cannot
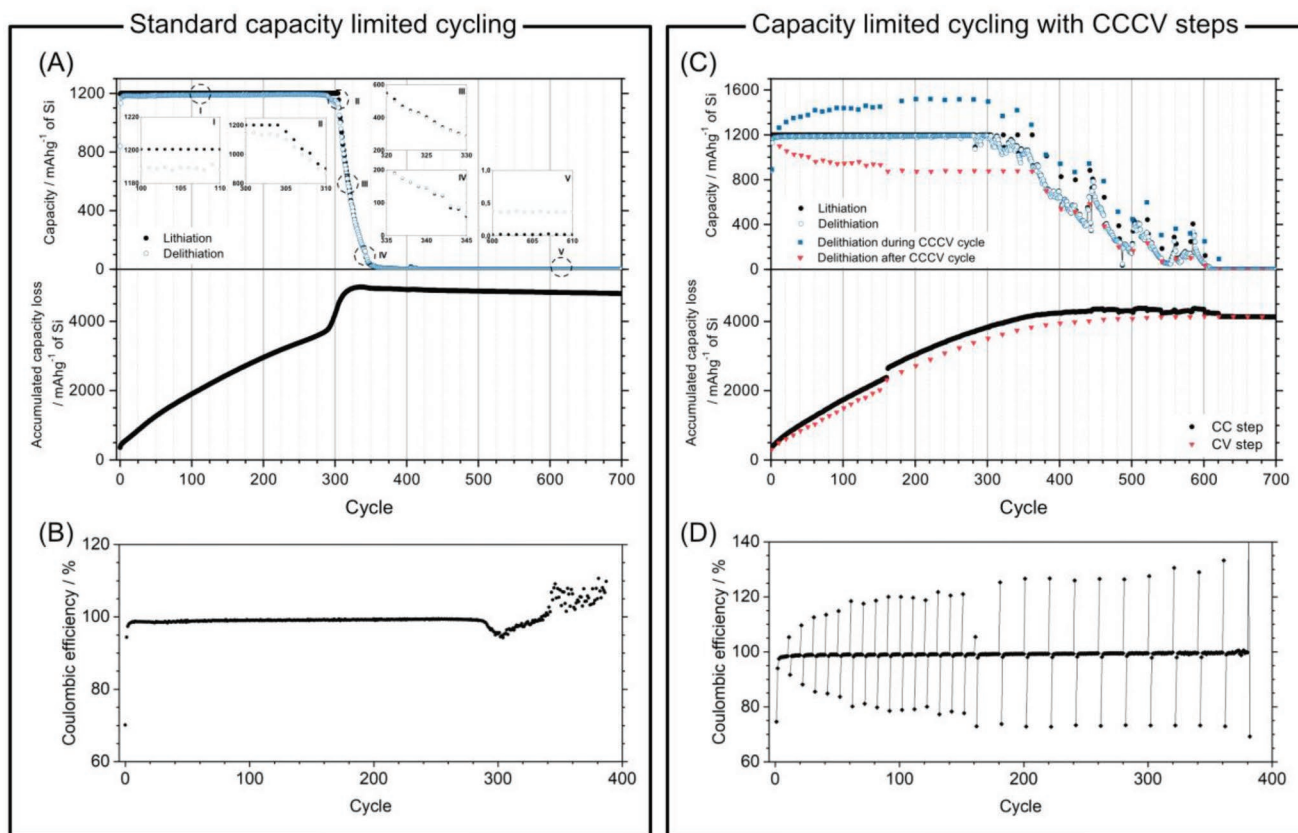
Figure 1. Capacity limited cycling for nanosilicon composite electrodes using A,B) standard cycling and C,D) constant current followed by constant voltage (i.e., CCCV) cycling. In (A) and (C), both the capacity and the accumulated capacity loss are shown as a function of the cycle number. The insets in (A) show magnified views of sections of the lithiation (black full circles) and delithiation (blue open circles) curves indicated by the letters I–V. In (B,D), coulombic efficiency versus cycle number plots are presented for both cycling procedures. The lower curves shows magnified view of the upper curves. The electrolyte was composed of 0.6 M lithium 4,5-dicyano-2-(trifluoromethyl)imidazolide (LiTDI) dissolved in dimethyl carbonate (DMC) and ethylene carbonate (EC) also containing fluoroethylene carbonate (FEC) and vinylene carbonate (VC). The volumetric electrolyte composition ratio was 2:1:0.1:0.02 with respect to DMC, EC, FEC, and VC, respectively.
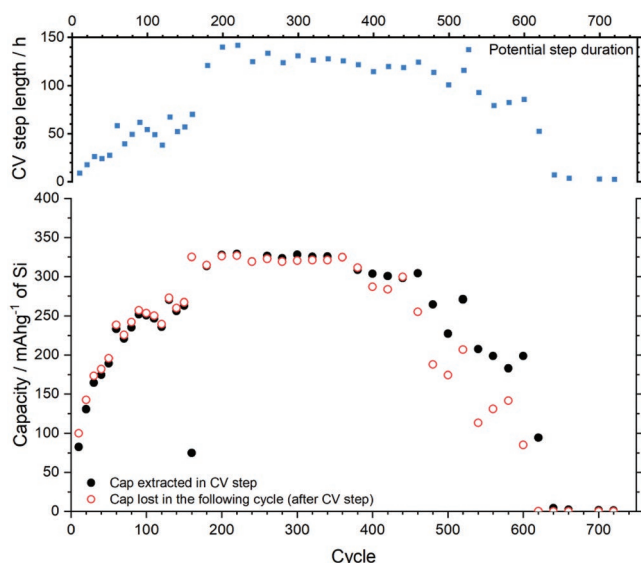
clearly be explained by SEI formation.[6] The capacity decrease seen in Figure 1A must, therefore, have stemmed from another phenomenon directly affecting the charge storage capacity of the silicon electrode. By plotting the accumulated capacity loss (i.e., the sum of the differences between the lithiation and delithiation charges) versus the cycle number, it can be seen (see Figure 1A) that the accumulated capacity loss (which was affected by the SEI formation charge) increased continuously to reach a maximum value of 4990 mAh g^{-1} after about 350 cycles. It is likewise evident that the increase was particularly large between the 290th and 320th cycles, i.e., where the marked drop in the coulombic efficiency was seen. At this stage, there was hence a dramatic change in the electrochemical performance of the electrode that resulted in a significantly decreased coulombic efficiency. More importantly, the increasing accumulated capacity loss did not affect the overall electrode performance as stable cycling capacity of 1200 mAh g^{-1} could be maintained during the initial 300 cycles. The experimental data, therefore, indicate that the silicon electrode gradually consumed its inherent capacity during the cycling even if this was not readily seen in the capacity versus cycle number plot. This demonstrates that capacity limited cycling does not solve the capacity loss problem but merely increases the number of useful cycles since the electrode is not allowed to undergo full lithiation. With capacity limited cycling, the electrode can thus be maintained functional for a relatively large number of cycles depending on the difference between the selected capacity limit and the theoretical capacity for the silicon electrode. Another important point is that while the accumulated capacity loss plot shows that the lithiation charge exceeded the delithiation charge during the first 300 cycles, the delithiation capacity exceeded the lithiation capacity later on during the cycling. The accumulated capacity loss, hence, started to decrease once the capacities of the electrodes had dropped to practically zero. This effect, which is more clearly seen in the coulombic efficiency versus cycle number in Figure 1B, is difficult to explain based on a degradation of the electrode due to volume expansion effects. Based on the data in Figure 1A,B, it is, therefore, reasonable to assume that the rapid capacity loss seen after about 300 to 350 cycles was coupled to the preceding increase in the accumulated capacity due to lithium trapping and SEI formation according to the hypothesis recently proposed by Rehnlund et al.[6]

The validity of the lithium trapping assumption can be further investigated by taking a closer look at the data in Figure 1. Since the capacity of the silicon electrode was at least 1200 mAh g^{-1} (i.e., 33% of the theoretical value) during 300 cycles, the effective coulombic efficiency, i.e., the coulombic efficiency for the capacity limiting reaction, z Li$^+$ + z e$^-$ + Si = Li$_z$Si, was 99.63%, as 0.9963^{300} ≈ 0.33. This effective coulombic efficiency can, hence, be regarded as the average coulombic efficiency for the abovementioned redox reaction in the absence of any superimposed irreversible reactions (not affecting the studied redox reaction). In the presence of such irreversible reactions, the coulombic efficiency should hence differ from 100% even when the lithiation and delithiation charges are identical. Since the effective coulombic efficiency (of 99.63%) was larger than the experimental coulombic efficiency (which was calculated for each cycle and varied between

97.3% and 99.4%), the present data consequently indicate the presence an irreversible reduction reaction. This is in excellent agreement with the fact that the apparent lithiation capacity would be given by the sum of the true lithiation charge and the charge due to the SEI formation. It is, therefore, difficult to predict the lifetimes of half-cells based on conventional coulombic efficiency values, which is illustrated as follows. Assuming a coulombic efficiency of 99%, only 5% of the initial capacity should have remained after 300 cycles (since 0.99^{300} = 0.05), although no significant capacity loss can be seen during the first 300 cycles in Figure 1A. More importantly, it can be concluded that the accumulated capacity loss must have been caused by at least two effects: an inability to completely oxidize the deposited lithium and SEI formation. Since the silicon electrode should be capacity limiting, the capacity decrease seen in Figure 1A must then have been caused by an inability to oxidize all the lithium deposited in the preceding lithiation step. This is in very good agreement with the diffusion controlled Li-trapping phenomenon recently described by Rehnlund et al.,[6] as well as the slow delithiation behavior previously described in the literature.[14]

Since the conventional constant current cycling results indicate that lithium was trapped in the silicon electrode as a result of an incomplete delithiation step, an alternative cycling scheme was used to investigate the possibility of increasing the delithiation efficiency by including a constant voltage delithiation pulse on every 10th delithiation step. As seen in Figure 1C, the capacity versus cycle number plot obtained with the latter CCCV cycling protocol shows that the capacity remained constant during the first 300 cycles in analogy with the conventional cycling results. In contrast to the rapid capacity decline seen after about 300 cycles during the conventional cycling, a more irregular and prolonged decline, extending to about 600 cycles, was, however, seen in the CCCV case. The accumulated capacity loss was also smaller in the CCCV case (i.e., about 4300 mAh g^{-1} as compared to about 5000 mAh g^{-1} for the CC cycling). The CCCV results consequently demonstrate that the lifetime of the silicon electrode could be prolonged considerably when the constant current delithiation step was complemented with a delithiation voltage step on every 10th cycle. This finding is difficult to explain based on SEI formation and volume expansion effects, since the experiments were carried out with analogous cells and as the only difference between the CC and CCCV protocols was the controlled voltage delithiation step used in the latter case. Since the lithium trapping effect should give rise to an increasing concentration of lithium in the electrode, the results instead indicate that the lifetime of the electrode can be extended by increasing the efficiency of the delithiation step. The latter is in excellent agreement with previous predictions.[6] The results, however, likewise indicate that the effect of the extra delithiation step was most pronounced when the silicon electrode was almost saturated with respect to lithium. This can be explained by an increased importance of the diffusion of lithium from the interior part of the electrode to the electrode surface once the electrode was almost saturated with lithium. As the CCCV results show that the efficiency of the delithiation process can be increased using a controlled voltage pulse, it is also reasonable to assume that the delithiation rate was limited by the lithium diffusion rate within the silicon electrode.

**ADVANCED
SCIENCE NEWS**
www.advancedsciencenews.com

**ADVANCED
ENERGY
MATERIALS**
www.advenergymat.de

Figure 2. The constant voltage-step-delithiation capacity and the capacity loss during the subsequent delithiation step as a function of the cycle number as well as a plot of the duration of the constant voltage step as a function of the cycle number.
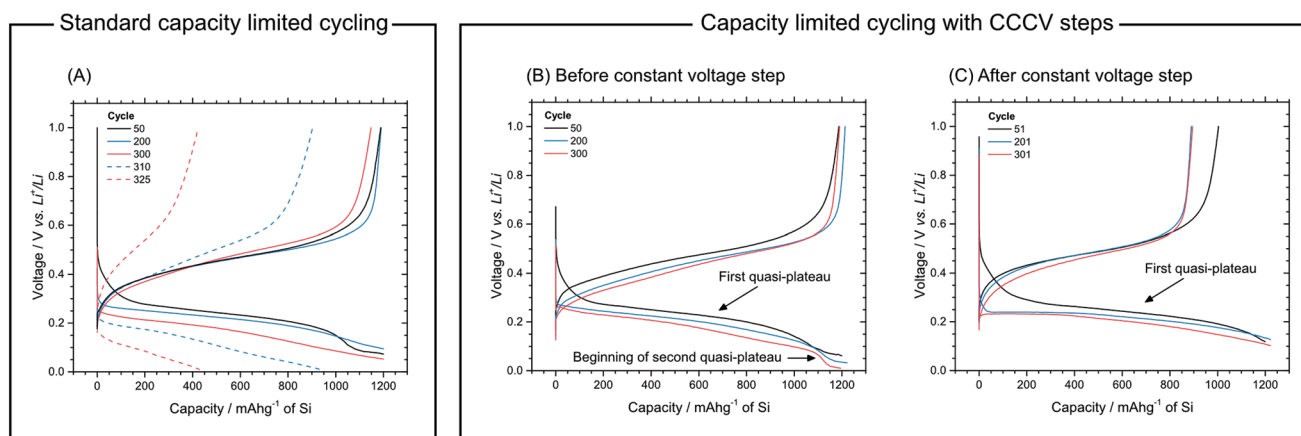
The impact of the constant voltage delithiation pulse can be studied in more detail using Figure 1C and **Figure 2**. During the first 200 cycles, the pulse delithiation capacity was found to increase to about 330 mAh g^{-1} after 200 cycles. Simultaneously, the time needed for the pulse current to decay to the cutoff current limit (i.e., 1 µA) increased from 9 to 140 hours due to the increasing concentration of lithium and the associated increase in the diffusion layer thickness of lithium in the electrode (see Section 2.6). The efficiency of the delithiation pulse can be estimated as follows: based on the data in Figure 1A, it can be assumed that a capacity of about 15 mAh g^{-1} was lost upon each cycle, which means that the capacity loss during the ten first cycles should have been about 150 mAh g^{-1}. A comparison of this value with the delithiation pulse capacity of about 80 mAh g^{-1} obtained on the 10th cycle indicates that about 55% of the capacity loss could be recovered with the delithiation pulse. A full recovery of the lost capacity was clearly not very likely as the length of the 10th cycle potential pulse was approximately nine hours while the total lithiation time during the first ten cycles was about 60 hours. In Section 2.2, the influence of the diffusion time on the capacity loss will be discussed in more detail. The abovementioned results, thus, indicate that it is possible to recover a significant fraction of the lost capacity using a complementary controlled voltage delithiation pulse and that this increases the lifetime of the silicon electrode.

However, as is seen in both Figures 1C and 2, the increase in the delithiation capacity obtained with the potential pulse was associated with a corresponding decrease in the delithiation capacity on the subsequent cycle, at least during about the first 350 cycles. This increased capacity for the lithiation cycle after the delithiation pulse cycle can be explained by the thicker lithium concentration profile generated for a longer delithiation step (see Section 2). This allows more lithium to be deposited during the following lithiation step compared to when the lithiation is carried out after a conventional constant current

delithiation step. Because of this, the lithium concentration profile present prior to the delithiation pulse should practically be restored. During the last 350 cycles a completely different behavior was, however, seen as the pulse delithiation capacity then generally exceeded the lithiation capacity on the subsequent cycle (see Figure 2). In this part of the experiment, a significant amount of lithium was consequently extracted from the electrode during each delithiation pulse although the reproducibility in the capacities was lower in this region than during the first 350 cycles. The occasional increases in the capacity due to increases in the delithiation charges could possibly be explained by increases in the electrode area due to the formation of cracks in the silicon particles. Such cracks would significantly facilitate the lithium diffusion and previously trapped lithium could then become accessible. The likelihood for a cracking of the nanoparticles would naturally increase with their lithiation degree, which could explain why this effect was not seen during the first 300 cycles. The resulting improved lithium extraction explains the relative slow capacity decay seen in this part of the CCCV cycling experiment in Figure 1C. The larger delithiation capacity (compared to the subsequent lithiation capacity) can be explained by lithium diffusing from the interior parts of the electrode toward the electrode surface. This is, hence, the opposite case compared to the behavior seen during the first 350 cycles when lithium was diffusing from the electrode surface toward the interior parts of the electrode.

After the CCCV cycling, the cell was disassembled in a glovebox and the lithium content in the silicon electrode was determined using ICP-AES (see the Experimental Section). Given that the electrode (composed of 3.140 mg silicon) was found to contain 2.574 mg lithium (see Table S1, Supporting Information), it is immediately clear that a large amount of lithium had been trapped in the electrode during the cycling. This confirms that the mismatch between the lithiation and delithiation capacities was indeed caused by the inability to fully oxidize the lithium deposited during the preceding lithiation step. As is described in more detail in Section 1, the ICP-AES data and the accumulated capacity loss indicate the formation of an alloy with an average composition of $Li_{3.28}Si$. The results further indicate that 99.5% of the lithium found in the electrode was present in the silicon electrode while the remaining 0.5% could be explained by lithium ions present in an SEI layer with an assumed thickness of 20 nm. As the lithium atoms in the lithium–silicon alloy could explain about 80% of the total accumulated capacity loss (see Figure 1C) it is also evident that the remaining 20% must have been associated with another process. As is described in Section 1, the latter capacity loss can be explained by the charge required to maintain a SEI layer with a thickness of 20 nm due to a continuous dissolution of the SEI layer during the cycling at a rate of about 0.2 nm h^{-1}. The elemental analysis data, which hence support the Li-trapping hypothesis,[6] consequently show that the main part (i.e., 80%) of the accumulated capacity loss stemmed from the incomplete delithiation step, in excellent agreement with the data in Figures 1 and 2.

Even though the ICP-AES results and the data in Figures 1 and 2 clearly show that the silicon electrode gradually became saturated with lithium during the cycling, it is still not immediately clear why this effect yields the capacity losses seen in

ADVANCED
SCIENCE NEWS
www.advancedsciencenews.com

ADVANCED
ENERGY
MATERIALS
www.advenergymat.de

Figure 3. Cycling curves for the indicated cycles obtained A) during standard constant current cycling, B) prior to a CCCV voltage step, and C) after a CCCV voltage step.

Figure 1. This point, however, can readily be explained using the cycling curves obtained with the standard and CCCV protocol, respectively. As can be seen in **Figure 3**, the standard cycling lithiation initially mainly involved the so called first quasi-plateau[3] as the second quasi-plateau was not reached until on the 50th cycle. Upon further cycling, a decrease in the lithiation potential was seen causing the quasi-plateaus to merge. In contrast, the shape of the delithiation curves remained essentially constant during the first 300 cycles. This difference between the shapes of the lithiation and delithiation curves can, therefore, not be explained by an increase in the interfacial resistance, e.g., due a growing SEI layer as this should affect the lithiation and delithiation steps equally. The experimental data also indicate that the thickness of the SEI layer remained practically constant during the cycling (see Section 2.3 as well as Section 1). According to Rehnlund et al.,[6] the shift in the lithiation potential is more likely to be associated with an increasing lithium surface concentration. As is described in more detail in Section 2.6, the lithium trapping effect should schematically result in the electrode becoming filled up in a process in which the trapped lithium appears to move toward the electrode surface. It is also likely that the lithium diffusion rate in the silicon electrode depends on the concentration of lithium in the electrode (see Section 1), in analogy with the behaviors seen for other electrodes.[18] It can consequently be expected that the lithiation step should become more and more difficult as the lithium concentration in the electrode is increasing. This is clearly seen in Figure S3 in the Supporting Information, depicting the cycling curves for cycles 400, 500, 600, and 700, respectively.

While the CCCV cycling protocol resulted in cycling curves with shapes similar to those obtained with the standard CC protocol, a significant difference was seen between the shapes of the cycling curves recorded before and after the constant voltage delithiation step (see Figures 3B,C as well as Figures S3–S5 in the Supporting Information). Prior to the constant voltage delithiation step, the cycling curve resembled the standard cycling curve exhibiting two distinguishable quasi-plateaus during the lithiation. After the constant voltage step, the lithiation curve, however, only featured the first quasi-plateau. In addition, a decreased lithiation overpotential was seen which resulted

in the lithiation terminating within the 0.15 to 0.1 V region compared to between 0.075 and 0.001 V prior to the constant voltage step. As previously explained, the lower delithiation capacity seen in Figure 3C can be explained by the effect of the preceding delithiation pulse. Based on the results in Figure 3 it can, therefore, be concluded that the delithiation pulse facilitates the subsequent lithiation via a decreased surface concentration of lithium in the electrode. The latter maintains the lithiation potential higher and hence the lithiation time longer (see Section 4) which allows the cycling to continue longer before the lithiation potential reaches the lithiation cut-off limit (i.e., the lithium plating potential).

Despite the decreased polarization during the lithiation step and the longer lifetime for the silicon electrode seen with the CCCV cycling protocol, it is immediately evident that the silicon electrode still failed. Based on the magnitude of the accumulated capacity losses (see Figure 1) and the ICP-AES results, this stemmed from the fact that the silicon electrode still became saturated with lithium because of lithium being trapped on each cycle. However, as previously mentioned, this is not expected since the delithiation pulse only was used on every 10th cycle. The gradual capacity losses seen in Figure 1 can, thus, be explained by the decrease in the lithiation potential (and hence the accessible lithiation cycling window) since the surface of the silicon electrode gradually was transformed into a lithium electrode surface. The different shifts in the CC and CCCV lithiation potentials were, incidentally, also unlikely to be due to changes in the overvoltages associated with the lithium counter electrode, the electrolyte and the separator (which also would affect the available cycling window) as analogous cells were used in the CC and CCCV cycling experiments. The main difference between the cycling behavior seen during the standard constant current and the CCCV cycling should, hence, have been caused by the differences in the lithium concentration in the surface region of the silicon electrode due to the delithiation step. As is evident from the cycling curves in Figure 3 and Figures S3–S5 in the Supporting Information, the decrease in the lithiation potential caused the CC capacity to drop to practically zero already after about 350 cycles whereas about 620 cycles was required to reach this point using the CCCV cycling scheme. This significant difference can be

explained based on the data in Figure 2 where it is seen that the effect of the delithiation pulse was particularly pronounced between approximately the 360th and 620th cycles. The lithiation potentials on cycles 400, 500, 600, and 700 thus remained above the lithiation cut-off limit for a longer period of time in the CCCV than in the CC experiments (see Figures S3–S5, Supporting Information).

Another difference between the CC and the CCCV capacity curves in Figure 1 concerns the dramatic increase in the accumulated capacity loss seen during the 290th to 320th cycles only in the CC case. As explained above, the results indicate that the surface concentration of lithium at this point became close to the saturation level during the lithiation step causing the lithiation cut-off limit to be reached earlier than in the CCCV case. This is further supported by the changes in the shapes of the lithiation curves as well as in the coulombic efficiencies seen in Figures 1 and 3. Note also that a dramatic decrease in the coulombic efficiency was found after about 290 cycles in the CC experiments whereas no such effect was seen in the CCCV case. As this sudden change in the coulombic efficiency suggests a change in the general lithiation, the delithiation behavior could be explained by elemental lithium deposition on the lithium saturated silicon surface. Lithium plating may also explain the rapid decrease in the lithiation potential seen between cycles 300 and 325 and the low coulombic efficiencies as such values often are obtained[19] for lithium deposition and oxidation in the present type of electrolyte. The large variation seen in the CC coulombic efficiencies after the 350th cycle can most likely be explained by the large uncertainties associated with the calculation of ratios between two values both being close to zero. It should be pointed out that lithium deposition on a lithium saturated silicon electrode very well could take place at a potential higher than 0 V versus Li+/Li as the latter standard potential merely refers to lithium deposition on a pure lithium electrode using a 1.0 M Li+ solution. On a silicon electrode saturated with lithium, the deposition would be expected to take place at a higher potential as the lithium activity in the silicon electrode would still not be expected to be equal to unity.[6]

As indicated above, the standard cycling lithiation potentials were generally more affected by the accumulation of lithium in the electrode than the delithiation potentials (see, e.g., Figure 3A). This is, however, not unexpected as a high lithium surface concentration should make a further lithiation more and more difficult based on the shift in the equilibrium potential discussed above, and as the diffusion of lithium should become less facile as the electrode surface becomes saturated with lithium. The delithiation step would, on the other hand, be expected to become more and more facile as the lithium concentration in the electrode is decreasing during this step. Once the electrode surface becomes saturated with lithium, the experimental results in Figure S3 in the Supporting Information, nevertheless, clearly show that the overpotential for the delithiation can become so large that the oxidation cut-off potential of 1.0 V versus Li+/Li is reached very quickly. This effect, which most likely stems from a low lithium diffusion rate in the electrode surface region, can therefore explain the decrease in delithiation capacity seen when the electrode is becoming saturated with lithium. The very low delithiation capacities seen for the almost fully lithiated silicon electrodes (see Figures S3–S5

in the Supporting Information) may then merely be ascribed to the inability of the electrodes to comply with the employed current densities as the electrodes clearly were full of lithium that should be able to undergo oxidation. As previously discussed,[6,18,20,21] the inherent asymmetry between the lithiation and delithiation reactions should make the lithiation step the rate-limiting step, in excellent agreement with the experimental results discussed in Section 2.4.

2.2. Diffusion Controlled Capacity Losses for Lithiated Silicon Electrodes

Based on the CC and CCCV cycling data combined with the ICP-AES results, it is immediately clear that a significant amount of lithium remained in the silicon electrode after the cycling and that this phenomenon involved elemental lithium diffusing into the silicon electrode. To study the influence of the diffusion in more detail a lithiated composite silicon electrode was subjected to a cycling protocol including open circuit pauses after the lithiation steps (which was carried out using the standard capacity limited cycling protocol described above). This was done to provide more time for the lithium diffusion process to proceed prior to the (constant current) delithiation step. In the first experiment comprising three cycles, a three-hour pause at the open-circuit potential (OCP) was employed between the lithiation and delithiation steps. The duration of the pause period was subsequently doubled after each experiment until the pause was 768 hours long. As can be seen in Figure S2 in the Supporting Information, the delithiation capacity was found to decrease when the duration of the pause was increased in good agreement with the behavior expected for a diffusion controlled process involving a porous electrode.[22] The delithiation capacity was, thus, found to depend linearly on the pause time raised to the power of 0.7. As indicated above, plots versus the time raised to the power of about 0.7 have been found to be appropriate for porous electrodes,[22] whereas plots versus the square root of time typically are seen for planar electrodes. Unfortunately, it was still not absolutely clear that the capacity loss was due to lithium diffusing into the electrode as another possibility could involve a diffusion controlled dissolution of the SEI layer, although the latter phenomenon is very unlikely to yield this type of capacity versus time plots with a time scale extending up to 768 hours. The influence of SEI formation on the capacity loss was, hence, further investigated as is explained below.

While it is challenging to estimate the capacity consumed by the SEI formation since this is superimposed on the silicon lithiation process, the analysis of the CCCV data (see Section 2.1 and Section S3 in the Supporting Information) indicated a SEI dissolution rate of about 0.1 nm h−1. Complementary to this approach, potential step experiments were employed to estimate the SEI dissolution rate in the absence and presence of the lithiation reaction. In these experiments, potential steps to 0.5 or 0.01 V, followed by a 6.25-hour long pause at the OCV, were first made until the capacities associated with the potential steps were stabilized (see Section S3 in the Supporting Information). The capacity consumed in the potential step to 0.5 V after the stabilization of the pulse capacity

(which was about 0.6 mAh g^{-1} cycle^{-1} after 50 cycles) was then assumed to represent the SEI dissolution. Analogously, the corresponding charge in the 0.01 V case (i.e., ≈2 mAh g^{-1} cycle^{-1} after 70 cycles) was assumed to be due to both lithium diffusion and SEI formation. These stabilized pulse capacities yield SEI dissolution rates of about 0.1 and 0.4 nm h^{-1}. Note that in the 0.01 V pulse experiment, the electrode should have become saturated with lithium to a larger extent than in the CCCV cycling as each deposition step was followed by a pause during which the lithium should have had the time to diffuse further into the electrode. As the potential steps to 0.01 V, therefore, were expected to give rise to an overestimated SEI dissolution rate, this estimate was instead based on the result of the 0.5 V potential step experiments. The latter indicate that the SEI dissolution rate was of the order of 0.1 nm h^{-1}, in good agreement with the calculations based on the CCCV data. Based on the latter SEI dissolution rate, it can then be deduced that the capacity loss of about 3.9 mAh g^{-1} seen during the first three-hour pause in the experiment depicted in Figure S1 in the Supporting Information mainly was due to lithium diffusing into the electrode. As the capacity of 0.6 mAh g^{-1} associated with the abovementioned SEI dissolution rate would correspond to about 15% of the capacity loss of 3.9 mAh g^{-1}, about 85% of the loss should hence have stemmed from the Li-trapping effect. The latter value is in good agreement with the 80% obtained based on the CCCV and ICP-AES data in Section 2.1. This further supports the conclusion that the accumulated capacity loss mainly stemmed from the lithium trapping effect.

In the previous Li-trapping study[6] using a pure LP40 electrolyte (i.e., 1 M LiPF$_6$ in EC:DEC 1:1), it was concluded that the SEI dissolution rate was about 1 nm h^{-1} and that ≈50% of the charge lost on each cycle stemmed from lithium trapping while 50% was caused by the SEI formation. The lower influence of the SEI effects seen here indicates that the use of the LiTDI electrolyte also containing VC and FEC (see Figure 1) did decrease the SEI dissolution problem significantly as intended. While the influence of the SEI problem could be decreased with the more optimized electrolyte used in this study, the results clearly demonstrate that the main factor affecting the capacity of the nanosilicon electrodes was the Li-trapping phenomenon. To decrease the capacity loss for silicon electrodes significantly, it is hence essential to decrease the influence of the trapping effect. As discussed previously[6] this may be done by selecting experimental conditions (e.g., very small particles immobilized on a conducting matrix with a large surface area) during which a full lithiation and delithiation of all particles can be attained. The present results, however, also indicate that it should be possible to slow down the increase in the lithium concentration in the electrode by increasing the efficiency of the delithiation step.

2.3. Hard X-Ray Photoelectron Spectroscopy (HAXPES) Analyses of Silicon Electrodes

The electrochemical and elemental analysis data strongly indicate that silicon electrodes suffer from capacity losses due to diffusion controlled lithium trapping and that the imbalance between the lithiation and delithiation charges is further increased by continuous SEI formation required to maintain a
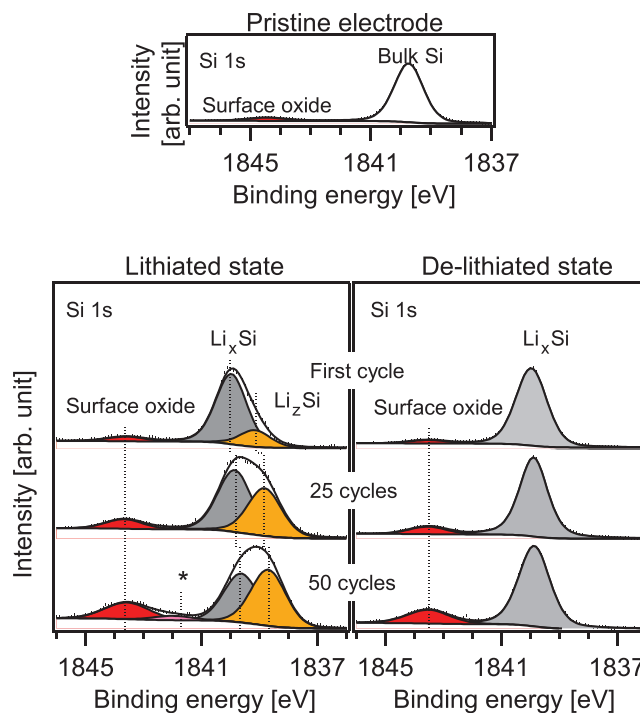
Figure 4. Si 1s HAXPES spectra for a pristine silicon electrode (top image) as well as lithiated and delithiated silicon electrodes (lower image) cycled for 1, 25, and 50 cycles, respectively, using the standard constant current approach described in Section 2.1.

constant thickness of the SEI layer. Although it is generally difficult to detect the trapped lithium using delithiated electrodes that only have been cycled for a few cycles, it should be possible to detect the trapped lithium at later stages in an extended cycling experiment. **Figure 4** shows hard X-ray photoelectron spectroscopy S1s spectra for a pristine silicon electrode as well as a silicon electrode analyzed after the lithiation and delithiation steps on the first, 25th and 50th cycles, respectively (the latter electrode was cycled using the standard constant cycling protocol discussed in Section 2.1). For the pristine electrode, two distinct peaks were observed due to the presence of silicon oxide and bulk Si, respectively. After the first lithiation, a new peak due to the Li–Si alloy emerged at lower binding energies (see the yellow Li$_z$Si peak in Figure 4) in addition to the silicon peak. In the spectra for the cycled electrode, the silicon peak was denoted Li$_x$Si to indicate that the electrode also contained some residual lithium yielding a shift toward lower binding energies.[23] The latter shift should, incidentally, be coupled to the shift in the redox potential of the electrode to lower potentials expected for an increasing lithium concentration in the electrode (see Section 2.1). After 25 and 50 cycles, the Li–Si alloy peak had clearly increased in size, indicating a build-up of residual lithium at the electrode surface that should not be present in the absence of the lithium-trapping effect. The latter is very important, as this is, to the best of our knowledge, the first HAXPES evidence for the lithium-trapping effect. By comparing the positions of the peaks in Figure 4 with those reported in our previous work involving step-by-step lithiation of silicon,[23] it can be seen that the spectra for the 25th cycle match those previously obtained using a lithiation capacity of

**ADVANCED
SCIENCE NEWS**
www.advancedsciencenews.com

**ADVANCED
ENERGY
MATERIALS**
www.advenergymat.de

2000 mAh g^{-1}. In addition, the spectra for the 50th cycle suggest a lithiation degree corresponding to a lithiation capacity between 2000 and 4000 mAh g^{-1}. Here it should be noted that the experimental data indicate that the silicon electrode should have had a total capacity (i.e., lithiation capacity + accumulated capacity loss) of 2055 and 2463 mAh g^{-1} after 25 and 50 cycles, respectively. It can, therefore, be concluded that the HAXPES results indicate that the lithium concentration in the electrode increases during the cycling in agreement with the electrochemical data and the lithium-trapping hypothesis.

Based on the significant accumulation of lithium in the electrodes indicated by the electrochemical data, the ICP-AES results and in the HAXPES spectra for the lithiated electrode, it could also be expected that the Li$_z$Si peak should be seen in the delithiated spectra. No such peak can, however, be seen in these HAXPES spectra in Figure 4. While this could indicate that the Li$_z$Si concentration, within the about 30 nm thick surface region probed in the HAXPES measurements, was too low after the 6.25-hour delithiation step, this explanation is unlikely since the spectra were recorded about seven days after the delithiation experiment. There should consequently have been sufficient time for lithium to diffuse from the internal parts of the electrode to the (delithiated) electrode surface. However, as this would generate a surface region in which all the probed silicon atoms had analogous lithium environments only one photoemission peak should be seen, in good agreement with the experimental results. The small shift in the Li$_x$Si peak toward lower binding energies with increasing cycle number hence constitute additional support for an increased lithium concentration in the delithiated electrodes.

2.4. Asymmetric Rate Cycling

The results discussed in Section 2.1 indicate that the delithiation step is inherently more facile than the lithiation step since the lithiation continuously increases the lithium concentration at the electrode surface. As such a behavior also was found by Li et al.,[20] the effect of asymmetric rate cycling on the capacity evolution of the present nanosilicon composite electrodes was studied using two types of experiments. In these experiments, the lithiation was either carried out at a "high" (i.e., 1000 mA g^{-1} or C/5 rate) or "low" (i.e., 50 mA g^{-1} or C/100 rate) rate followed by delithiation at a low or high rate for 25 cycles after which the opposite conditions were applied for 25 cycles as shown in **Figure 5**. In the discussion below, these two protocols will be referred to as the "fast lithiation" and "slow lithiation" protocols, respectively. With the fast lithiation approach (see Figure 5A) a large capacity drop was seen on the first two cycles followed by an increase during the subsequent eight cycles (most likely due to an increase in the electroactive electrode area due to volume expansion effects[6]) after which the capacity dropped dramatically to close to zero (i.e., ≈2 mAh g^{-1}). A lithiation capacity of about 3640 mAh g^{-1} (corresponding to about 95% of the first cycle lithiation) was, however, still obtained immediately after switching to the slow lithiation and fast delithiation protocol. During the subsequent cycling, the capacity decreased almost linearly with the cycle number to reach about 1200 mAh g^{-1} after 50 cycles. The plot of the accumulated capacity loss versus the
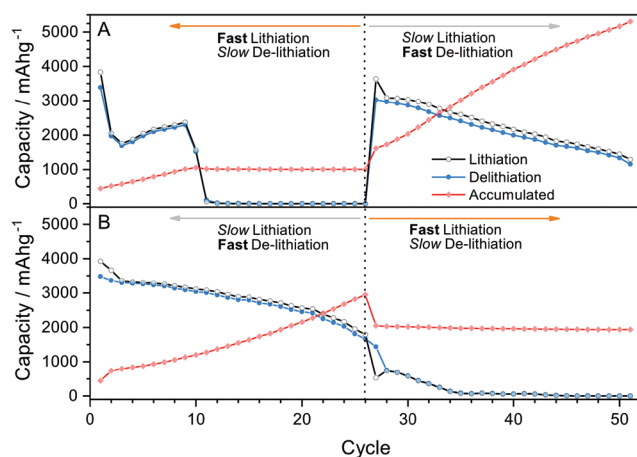
Figure 5. The lithiation and delithiation capacities as well as the accumulated capacity loss as a function of the cycle number for two nanosilicon-based half-cells subjected to asymmetric cycling. This cycling involved A) fast lithiation and slow delithiation for 25 cycles followed by slow lithiation and fast delithiation for another 25 cycles and B) slow lithiation and fast delithiation for 25 cycles followed by fast lithiation and slow delithiation for another 25 cycles.

cycle number, also included in Figure 5A, demonstrates that the capacity loss on the first cycle was of the order of 500 mAh g^{-1} and that the major increase in the accumulated capacity loss was seen during the slow lithiation part of the cycling. The accumulated capacity increase rate was thus clearly lower in the fast lithiation case compared to the slow lithiation case. The results obtained with the slow lithiation protocol (see Figure 5B), hence, further support the asymmetric lithiation and delithiation hypothesis as the results confirm that a slow lithiation gives rise to higher capacities but also a rapidly increasing accumulated capacity loss, while the capacity drops close to zero as soon as fast lithiation is employed. The latter causes the lithium concentration at the electrode surface to increase rapidly which leads to an early termination of the lithiation when the lithiation cut-off limit is reached. One interesting difference between the behavior in Figure 5A and B is that there was a decrease in the accumulated capacity loss when going from slow lithiation to fast lithiation on cycle 26 in Figure 5B. The latter indicates that the delithiation step is inherently faster than the lithiation step which is in agreement with the findings of Li et Al.[20] and the conclusions in Section 2.1.

The results in Figure 5, thus, show that the slow lithiation protocol yields high capacities but also a rapid increase in the accumulated capacity loss due to the fast delithiation step. To minimize the accumulated capacity loss, the delithiation step should therefore be longer than the lithiation step in good agreement with the CCCV results discussed in Section 2.1. Conversely, the fast lithiation protocol offers a more complete delithiation (due to the longer delithiation step) but also low capacities due to the rapid increase of the lithium concentration at the electrode surface. The capacity of these silicon electrodes was consequently limited by the lithiation step while the delithiation step, albeit inherently faster than the lithiation step, clearly was incomplete. As a result, the concentration of lithium in the electrode gradually increased which slowly converted the silicon electrode into a silicon electrode with (at least) the

surface almost saturated with lithium. One way to slow down this process is to employ the CCCV approach employed in Section 2.1 in which the delithiation efficiency is increased via the inclusion of controlled voltage delithiation pulses. As the rate of the delithiation step should be limited by the diffusion rate of lithium in the silicon electrode, controlled voltage rather than controlled current pulses are best used to increase the delithiation efficiency. A sufficiently slow lithiation step followed by an even slower delithiation step should hence be used to obtain a high capacity and to minimize the capacity loss due to lithium trapping, respectively.

2.5. Capacity Loss Mechanisms

Even though the experimental conditions used in this study were chosen to minimize the cycling capacity losses, it is immediately clear from the experimental results that the adopted strategy failed to solve this problem. The aim of the present work is, therefore, to identify the main effect responsible for the capacity losses and to address some important remaining issues related to the lithium-trapping hypothesis using complementary experimental approaches, including pulsed open circuit experiments and ICP-AES and HAXPES analyses of cycled electrodes. As mentioned in the introduction, several phenomena are often used to explain the capacity decay generally seen for silicon electrodes. The most commonly discussed phenomena will, therefore, be discussed below in the light of the present experimental results.

While repeated volume variations giving rise to a loss of active material is a frequently proposed explanation, this explanation appears unlikely as nanoparticles are known to be able to handle volume expansion effects without breaking.[12] Previous scanning electron microscopy (SEM) investigations of cycled silicon electrodes have likewise failed to detect any significant cracking of the composite electrode or loss of the active material.[24] It is also not clear why volume expansion effects would give rise to the diffusion-controlled capacity loss effect described in Section 2.2, especially as the influence of the volume expansion effects should have been very small during the open circuit pauses used in this experiment. The experimental data discussed in Section 2.1 are likewise difficult to explain based on the volume expansion hypothesis as different results were obtained with the same type of silicon electrodes using two different cycling protocols only differing with respect to an additional controlled voltage delithiation step applied on every 10th cycle. The HAXPES results also indicate that no highly lithiated phases remained in the surface region of the electrode after the delithiation step, which could suggest that parts of the electrode material had been made electrochemically inactive during the cycling. Due to abovementioned points, it can be concluded that a loss of active material due to volume expansion effects is very unlikely to be the main reason for the observed capacity losses.

In another commonly suggested capacity loss mechanism it is assumed that a growing SEI layer gives rise to an increased cell resistance that results in the cut-off values being reached prematurely. As the latter gives rise to a decreased capacity, much effort has consequently been made to optimize

the properties of the SEI layer to circumvent this problem. One major problem with this hypothesis is that it does not offer a straightforward explanation for the significant amounts of lithium found in the ICP-AES analysis of the cycled silicon electrode. Another issue concerns the fact that the iR drop across the SEI layer should affect both the lithiation and delithiation potentials while the cycling curves in Figure 3A mainly show an increased polarization during the lithiation steps (an effect that incidentally may be explained based on the increasing lithium concentration in the electrode). Analogous observations regarding the shapes of the cycling curves were also discussed in our previous publications.[24,25] Moreover, it is not clear why the capacity losses in Figures 1A,C were only seen after about 300 cycles given that the SEI is known to be formed during the initial cycles. No experimental evidence was likewise found suggesting an increasing thickness of the SEI layer as the electrochemical and the HAXPES data indicate that the thickness of the SEI layer remained approximately constant after the first few cycles. The differences between the results in Figure 1 obtained with the two cycling protocols (and analogous cells) is likewise difficult to explain on the basis of an increase in the resistance of the SEI layer during the cycling. Here it should also be pointed out that the mass transport related resistance of the SEI layer with respect to the lithium deposition and oxidation reactions, in fact, should be rather low as Li$^+$ ions readily can pass through this layer. The corresponding mass transport related resistance with respect to the reduction of the solvent should, on the other hand, be significantly higher as the diffusion of the solvent in the SEI layer should be slow. To exclude a further reduction of the solvent at the interface between the SEI and the electrolyte, the electronic conductivity of the SEI layer must clearly be low enough. This means that with respect to lithium deposition and oxidation reactions, the SEI layer can consequently be regarded as a solid electrolyte layer. Given its typical thickness of less than 20 nm it is then unlikely to give rise to a significant iR drop even if one assumes that the Li$^+$ mobility is much lower in the SEI than in the much thicker electrolyte filled separator. This indicates that the present capacity losses were very unlikely to be due to an increasing iR drop caused by an increase in the thickness of the SEI layer.

A capacity loss due to the charge involved in the SEI formation can likewise be excluded since the present experiments were made with half-cells containing lithium counter electrodes.[6] This effect can neither explain the differences seen in Figure 1 for the two different cycling approaches, nor the results discussed in Section 2.2.

As discussed in connection with the experimental results, the capacity loss observed with the present nanosilicon composite electrodes can, on the other hand, readily be explained based on the recently proposed lithium-trapping model.[6] In the latter, the incomplete delithiation step is assumed to be caused by lithium diffusing from the electrode surface toward the inner parts of the electrode making a small part (i.e., less than 1%) of the deposited lithium inaccessible during the delithiation step, as is described in detail in Section 2.6. The cycling behavior and capacity losses observed in the different experiments using the present silicon electrodes are readily explained by such a gradual build-up of the lithium concentration in the electrode, which also was verified by the ICP-AES results

**ADVANCED
SCIENCE NEWS**
www.advancedsciencenews.com

**ADVANCED
ENERGY
MATERIALS**
www.advenergymat.de

obtained for the CCCV cycled electrode. Diffusion controlled trapping of lithium in the electrode as previously proposed[6] is likewise in good agreement with the observed accumulated capacity loss. This can be explained based on the charge associated with the deposition of the trapped lithium and the charge needed to maintain a 20 nm SEI layer assuming a slow (i.e., about 0.1 nm h^{-1}) dissolution of the latter. The gradual saturation of the electrode surface with respect to lithium can likewise explain the gradual decrease in the lithiation potential that often is assumed to be caused by an increasing iR drop in the SEI layer. Here it should be pointed out that the lithium trapping capacity loss should be seen independent of whether the experiments are carried out using controlled current or controlled voltage methods. The latter is in excellent agreement with previous results[6,26] indicating that the time available for the lithium diffusion depends on the voltage window employed in controlled voltage cycling experiments. Another important result is that the diffusion-controlled capacity loss seen during the open circuit periods after the lithiation of the electrode discussed in Section 2.2, indicate that lithium is diffusing from the electrode surface toward the inner part of the electrode as a result of the concentration gradient formed during the lithiation step. The CCCV results also clearly show that the trapped lithium can be released if the time domain of the delithiation step is extended, e.g., using a controlled voltage rather than galvanostatic delithiation step. The inherent asymmetry between the lithiation and delithiation steps, e.g., illustrated by the fact that the delithiation step is inherently faster than the lithiation step, is another consequence of the accumulation of lithium in the electrode during the lithiation step. The lithium-trapping model is, therefore, the only present model able to explain the capacity losses seen in the present work as well as in the previous work by Rehnlund et al.[6] This model will, therefore, be described in more detail in the following section.

2.6. Lithium Trapping in Nanosilicon Composite Electrodes

In our previous work,[6] lithium trapping in silicon electrodes was demonstrated to give rise to a fast capacity decay during the first 100 cycles under full-capacity cycling conditions. In the present case, a significant capacity loss was only seen after about 300 cycles using capacity limited cycling involving 33% of the theoretical capacity. This difference, which merely stems from the about three times lower accumulation rate of lithium in the electrode, can be explained based on the schematic illustration in **Figure 6**. Under full capacity cycling conditions, the lower cut-off limit of 0.01 V versus Li$^+$/Li is reached when the lithium concentration at the silicon electrode surface approaches the saturation limit. This gives rise to a lithium
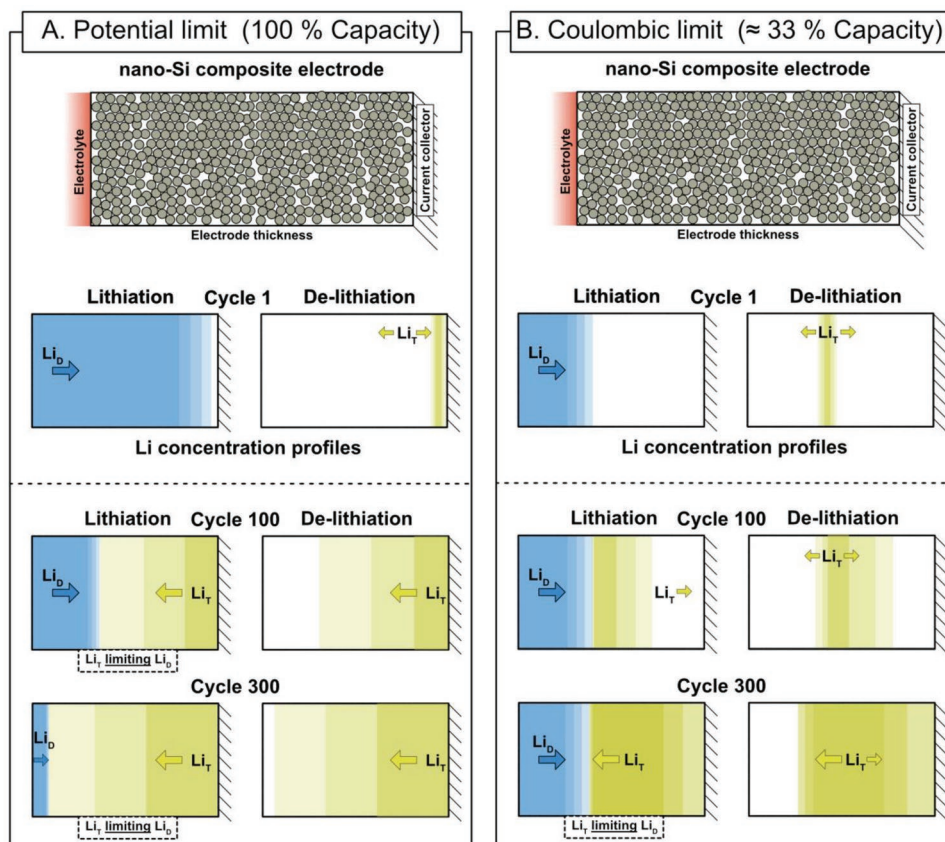
Figure 6. Schematic representation of the lithium concentration profiles inside the silicon electrode during different stages of the cycling using A) controlled voltage full capacity cycling and B) coulombic limited cycling protocol. The lithium concentration profiles are shown for the deposited lithium (Li$_D$ in blue) and trapped lithium (Li$_T$ in yellow) while the arrows indicate the lithium diffusion directions.

**ADVANCED
SCIENCE NEWS**
www.advancedsciencenews.com

**ADVANCED
ENERGY
MATERIALS**
www.advenergymat.de

concentration gradient and hence diffusion toward the inner parts of the electrode where the lithium concentration is lower. During the delithiation step, the lithium therefore diffuses not only toward the electrode surface where the oxidation takes place but also toward the internal parts of the electrode. Even though almost all of the deposited lithium is oxidized, this phenomenon results in a small fraction of the deposited lithium (i.e., less than 1%) to remain in the electrode, at least when the delithiation time is similar to the lithiation time. The latter is a result of the fact that, under constant current conditions, the duration of the delithiation step is controlled by the time during which the lithium diffusion rate toward the electrode surface is able to support the applied current. On each cycle, a small amount of lithium hence escapes oxidation during the delithiation step in agreement with the gradual increase seen in the accumulated charge and the ICP-AES results obtained after the CCCV cycling experiment. As the lithium concentration in the electrode gradually increases, the capacity of the electrode becomes lower and lower as less and less lithium needs to be deposited to reach the cut-off limit. The fact that the lithiation potential decreases during the cycling can then be explained based on a decrease in the lithiation equilibrium potential and an increased lithium mass transport related resistance caused by the fact that the diffusion rate of lithium should decrease as the lithium concentration in the electrode increases.

During capacity limited cycling conditions there is likewise a gradual increase in the lithium concentration in the electrode but in this case the influence of the effect remains practically invisible for many more cycles due to the fact that the full capacity of the electrode is not used meaning that the lithium trapping rate is lower. The delithiation step is, thus, still incomplete which results in a small amount of trapped lithium in the silicon electrode. As the cycling continues, the electrode is initially able to store the designed amount of Li_D (e.g., the amount corresponding to 33% of the theoretical capacity for silicon) without any interference from the Li_T zone. However, at some point (i.e., after about 300 cycles for the present 33% capacity cycling), this changes and the capacity starts to drop in analogy with the behavior seen during the full capacity cycling conditions. It can, therefore, be concluded that the limited capacity cycling approach merely prolongs the lifetime of the silicon electrode at the expense of a decreased cycling capacity.

3. Conclusions

The results presented here clearly show that the capacity fading seen for the present silicon nanoparticle-based electrodes, which were cycled in half-cells containing lithium-metal counter electrodes, was caused by a gradual increase in the lithium concentration in the electrode. The latter effect, which stemmed from a small fraction of lithium being trapped in the electrode on each cycle, is evident from the ICP-AES determination of the lithium concentration in the cycled electrode (indicating a final Li:Si mol-ratio of 3.28) and the calculations based on the accumulated capacity losses seen in the experiments. While the use of capacity limited cycling (using a cycling capacity of 1200 mAh g^{-1}) allowed the cell to cycle 300 cycles, this effect was merely due to a decreased lithium-trapping rate as less

lithium was deposited on each lithiation cycle. The capacity loss can be explained by the increasing lithium concentration in the silicon electrode since less and less lithium would be needed to be deposited to reach the preset lithiation cut-off limit during the controlled current lithiation conditions. The underlying problem is that during the delithiation step there will be diffusion of lithium not only toward the electrode surface, but also toward the inner parts of the electrode if the lithium concentration still is lower there. The latter means that a small fraction (typically <1%) of the deposited lithium can become trapped in the electrode upon each cycle, at least under symmetric cycling conditions, i.e., when the durations of the lithiation and delithiation steps are similar.

While the analyses of the accumulated capacity losses demonstrate that about 80% of the capacity loss stemmed from the lithium trapped in the electrode, the data also show that the remaining loss (i.e., 20%) was caused by SEI formation due to dissolution of the SEI layer at a rate of about 0.1 nm h^{-1}. While the SEI formation affected the coulombic efficiency and hence clearly also would affect the capacity of a full cell, the SEI formation did not affect the capacity of the present silicon electrode–based half-cells since the SEI charge was compensated for by the lithium-metal counter electrode. While the present results clearly demonstrate that lithium trapping is a very important capacity-limiting phenomenon for silicon electrodes, it is likewise reasonable to assume that the effect is present also for other lithium-alloy forming electrode materials. As the influence of the trapping effect is caused by lithium diffusing in the electrodes and the obtained lithium concentration profiles, its influence should depend, e.g., on the lithiation and delithiation times, the thickness of the electroactive material (i.e., the maximum lithium diffusion length), and the temperature.

The results also indicate that the mass transport resistance in the silicon electrode increases as the lithium concentration in the electrode increases. The latter effect is clearly most pronounced at the electrode surface during the lithiation step, which also means that an increase in the lithiation rate results in a decreased capacity as the results also show that the capacity of the silicon electrode is controlled by the lithiation reaction. During the cycling, the silicon electrode, in fact, becomes more similar to a lithium electrode as the concentration of lithium in the electrode increases. As the lithiation potential should depend on the activity of lithium in the silicon electrode, this effect and the increased mass transport resistance shift the lithiation reaction to a lower potential. The cut-off limit is then reached faster, and the capacity consequently decreases. During the lithiation step, the surface concentration of lithium should always be higher than the lithium concentration in the internal part of the electrode, causing lithium to diffuse into the electrode. If the lithiation rate is too high or the lithium diffusion rate at the surface of the electrode becomes too low, the electrode surface would essentially become identical to that of a lithium-metal electrode. This would result in the potential reaching the lithiation cut-off limit, which is typically set to avoid lithium plating.

The comparison between the standard constant current cycling protocol (CC) and constant current cycling with intermittent constant voltage delithiation steps (CCCV) indicate that the latter protocol gave rise to a significantly improved cycling performance as some of the trapped lithium was released

**ADVANCED
SCIENCE NEWS**
www.advancedsciencenews.com

**ADVANCED
ENERGY
MATERIALS**
www.advenergymat.de

during the constant voltage delithiation steps. The latter results demonstrate that it is possible to at least slow down the rate of the capacity loss by increasing the efficiency of the delithiation step, i.e., by using sufficiently long constant voltage delithiation steps. While a frequent inclusion of such delithiation steps should increase the lifetime and overall performance of silicon electrodes significantly, such approaches may even pave the way for regeneration of consumed batteries.

Stable capacities for silicon electrodes (as well as other lithium alloy forming compounds) should be possible to obtain if the delithiation charge can be made equal to the lithiation charge on each cycle. The results presented here indicate that this requires that the duration of the delithiation step is made longer than that of the lithiation step. An alternative approach could be to use electrodes in which a full lithiation and delithiation can be obtained during each cycle. However, this would most likely require the use of rather porous electrode containing surface confined silicon nanoparticles, which unfortunately would exhibit rather low volumetric capacities. The CCCV approach presented in this work, therefore, seems to constitute a more versatile strategy, particularly if the constant voltage steps are used more frequently than in this work. This proof-of-principle work, therefore, paves the way for new approaches for the realization of silicon-based electrodes with significantly extended lifetimes as well as methods allowing the regeneration of degraded electrodes.

4. Experimental Section

The composite Si electrodes were composed of Si nanoparticles ($\approx$100–200 nm), carbon black (CB) (Super P, Erachem Comilog), and Na-carboxymethyl cellulose (CMC) (D.S = 0.90: MW = 700 000 g mol^{-1}, Sigma Aldrich). The dry components were first mixed in a pH 2.8 buffer solution containing KOH and citric acid (CA). Further mixing was then carried out with a planetary ball mill (Retsch PM44) for one hour to produce a homogenous mixture. The mixture was then bar-coated on a 20 μm thick Cu foil and dried at 60 °C in air. The dry coating consisted of 67% Si, 10% CB, 7% CMC, 14% CA, and 2% KOH. Circular electrodes with a diameter of 20 mm were obtained by a Hohsen punching tool resulting in an average Si mass loading of 1.0 mg cm^{-2}. The reported specific capacities and current densities were calculated using the mass of the silicon in the electrodes. Prior to half-cell assembly, the electrodes were dried in an argon-filled glovebox at 120 °C under vacuum.

Half-cells, sealed in a plastic-coated aluminum pouch under vacuum, were assembled using a Solupor separator (DSM) and a Li foil counter electrode. The electrolyte consisted of 0.6 M lithium 4,5-dicyano-2-(trifluoromethyl)imidazolide (LiTDI) dissolved in dimethyl carbonate (DMC) and ethylene carbonate (EC) (BASF selectilyte) with additions of fluoroethylene carbonate (FEC) (Sigma-Aldrich) and vinylene carbonate (VC) (Vinylene carbonate E, BASF). The volumetric electrolyte composition ratio was 2:1:0.1:0.02 with respect to DMC, EC, FEC, and VC, respectively.

Galvanostatic cycling was performed using a Digatron BTS 600 galvanostat. The first cycle was performed with a current corresponding to a current density of 48 mA g^{-1} (Si) while the subsequent cycles involved a current density of 192 mA g^{-1} (Si). The lithiation capacity was limited to 1200 mAh g^{-1} (Si) (i.e., 1.2 mAh cm^{-2} (Si)) while the lithiation and delithiation cut-off limits were set to 0.01 and 1.0 V versus Li$^+$/Li, respectively. In the cycling involving the constant voltage steps (i.e., the CCCV cycling), the voltage during the constant voltage pulse was fixed at 1.0 V and the oxidation current was measured until the current dropped below 1 μA. The voltage pulses were employed after the first cycle and then after every 10th cycle up till the 160th cycle, and subsequently after every 20th cycle.

To determine the self-discharge rate during the capacity limited cycling procedure, a half-cell was first cycled according to the capacity limited cycling scheme for 50 cycles to reach a stable performance. The half-cell was, thereafter, lithiated using a capacity of 1200 mAh g^{-1} (Si) after which the half-cell was allowed to rest under open circuit conditions for a three-hour period. Subsequently, a standard delithiation step was first carried out followed by two full standard cycles employed to restore the normal function. This cycling scheme was then repeated with a continuous doubling of the rest period until the latter reached a length of 768 h.

To estimate the capacity consumed due to continuous SEI formation as a result of SEI dissolution, a potential step cycling sequence was applied. First, a constant current density (0.48 mAh g^{-1} (Si)) was applied until a cell voltage of 0.5 V versus Li$^+$/Li was reached, where very little lithiation of the silicon should take place. The latter cell voltage was then maintained for 25 h followed by an equally long open circuit pause. After this, another potential step to 0.5 V was applied but for 6.25 h followed by an equally long pause. The 6.25-h potential step and 6.25-h pause sequence was then repeated for 100 cycles. A similar potential step scheme involving a cell voltage of 0.01 V was also used in another experiment. In the latter case, the first potential step to 0.01 V was followed by a 100-h pause at open circuit. After this, a potential step to 0.01 V for 6.25 h was followed by an equally long pause, and this procedure was then repeated for 100 cycles. Note that in the 0.01 V case there should be both lithiation of the silicon electrode and SEI formation.

The asymmetric cycling protocol consisted of an initial cycle of "slow" lithiation/delithiation at 50 mA g^{-1} for the first. Cycle 2–26 continued with fast lithiation cycling at "high" (i.e., 1000 mA g^{-1} or C/5 rate) and slow delithiation at "low" (50 mA g^{-1} or C/100 rate). The opposite conditions were applied for the next 25 cycles with slow lithiation and fast delithiation. In order to rule out any possible effect of which order the protocol was applied, two identical cells were run with mirrored asymmetric protocols.

The amounts of lithium present in the silicon composite electrodes after CCCV cycling were determined as follows. The electrodes were first washed three times in dimethyl carbonate (DMC) to remove traces of the electrolyte. The electrodes were then carefully exposed to water to extract most of the lithium. This gave rise to a vivid reaction (i.e., 2 Li + 2 H$_2$O = 2 Li$^+$ + 2 OH$^-$ + H$_2$) and the formation of a brownish gel-like precipitate, most likely containing the silicon particles and the other components of the composite electrode. The copper current collectors were removed, rinsed with MQ-filtered ultrapure water, and subsequently dissolved in HNO$_3$ after which the amounts of lithium in the solutions were determined as described above. The solutions containing the precipitates were treated with 10% HNO$_3$ and centrifuged and the amounts of lithium in the supernatants were determined. The precipitate was first digested until dryness three times using a mixture of 3.0 mL of HNO$_3$ and 1.0 mL HF. Since this did not result in a complete dissolution of the precipitate, the lithium determination was carried out by introducing the slurry, most likely containing graphite particles, directly into the ICP-AES instrument. As the graphite particles were completely atomized in the plasma, the amount of lithium in the precipitate could still be determined.

The HAXPES measurements were performed at the HIKE end station at the KMC-1 beamline at the synchrotron facility BESSY II operated by the Helmholtz-Zentrum Berlin. The samples were opened in an argon-filled glovebox, rinsed in DMC, and mounted on the sample holder using conductive Cu-tape. Sample transfers to the analysis chamber were made without air exposure. The Si1s spectra were calibrated to place the main oxide peak at 1843.6 eV except for the pristine Si electrode in which case the position of the oxide peak was adjusted to 1844.4 eV.

Supporting Information

Supporting Information is available from the Wiley Online Library or from the author.

[1] J. B. Goodenough, Y. Kim, *Chem. Mater.* **2010**, *22*, 587.

[2] H. Li, Z. X. Wang, L. Q. Chen, X. J. Huang, *Adv. Mater.* **2009**, *21*, 4593.

[3] M. N. Obrovac, V. L. Chevrier, *Chem. Rev.* **2014**, *114*, 11444.

[4] E. Peled, *J. Electrochem. Soc.* **1979**, *126*, 2047.

[5] M. Gauthier, T. J. Carney, A. Grimaud, L. Giordano, N. Pour, H.-H. Chang, D. P. Fenning, S. F. Lux, O. Paschos, C. Bauer, F. Maglia, S. Lupart, P. Lamp, Y. Shao-Horn, *J. Phys. Chem. Lett.* **2015**, *6*, 4653.

[6] D. Rehnlund, F. Lindgren, S. Böhme, T. Nordh, Y. M. Zou, J. Pettersson, U. Bexell, M. Boman, K. Edström, L. Nyholm, *Energy Environ. Sci.* **2017**, *10*, 1350.

[7] H. Kim, E.-J. Lee, Y.-K. Sun, *Mater. Today* **2014**, *17*, 285.

[8] J. H. Ryu, J. W. Kim, Y.-E. Sung, S. M. Oh, *Electrochem. Solid-State Lett.* **2004**, *7*, A306.

[9] M. N. Obrovac, L. Christensen, *Electrochem. Solid-State Lett.* **2004**, *7*, A93.

[10] U. Kasavajjula, C. Wang, A. J. Appleby, *J. Power Sources* **2007**, *163*, 1003.

[11] a) J. Graetz, C. C. Ahn, R. Yazami, B. Fultz, *Electrochem. Solid-State Lett.* **2003**, *6*, A194; b) H. Li, X. Huang, L. Chen, Z. Wu, Y. Liang, *Electrochem. Solid-State Lett.* **1999**, *2*, 547; c) N. Liu, Z. Lu, J. Zhao, M. T. McDowell, H.-W. Lee, W. Zhao, Y. Cui, *Nat. Nanotechnol.* **2014**, *9*, 187; d) D. L. Ma, Z. Y. Cao, A. M. Hu, *Nano-Micro Lett.* **2014**, *6*, 347.

[12] X. H. Liu, L. Zhong, S. Huang, S. X. Mao, T. Zhu, J. Y. Huang, *ACS Nano* **2012**, *6*, 1522.

[13] B. Jerliu, L. Dorrer, E. Huger, G. Borchardt, R. Steitz, U. Geckle, V. Oberst, M. Bruns, O. Schneider, H. Schmidt, *Phys. Chem. Chem. Phys.* **2013**, *15*, 7777.

[14] a) H. Li, X. J. Huang, L. Q. Chen, G. W. Zhou, Z. Zhang, D. P. Yu, Y. J. Mo, N. Pei, *Solid State Ionics* **2000**, *135*, 181; b) F. Wang, L. J. Wu, B. Key, X. Q. Yang, C. P. Grey, Y. M. Zhu, J. Graetz, *Adv. Energy Mater.* **2013**, *3*, 1324; c) V. A. Sethuraman, V. Srinivasan, J. Newman, *J. Electrochem. Soc.* **2013**, *160*, A394; d) S. W. Lee, H.-W. Lee, I. Ryu, W. D. Nix, H. Gao, Y. Cui, *Nat. Commun.* **2015**, *6*; e) T. Yoon, C. C. Nguyen, D. M. Seo, B. L. Lucht, *J. Electrochem. Soc.* **2015**, *162*, A2325.

[15] a) J. Yang, M. Wachtler, M. Winter, J. O. Besenhard, *Electrochem. Solid-State Lett.* **1999**, *2*, 161; b) L. Liu, M. N. Obrovac, *ECS Electrochem. Lett.* **2012**, *1*, A10; c) P. P. Ferguson, R. A. Dunlap, J. R. Dahn, *J. Electrochem. Soc.* **2010**, *157*, A326; d) Z. Huang, S. Hu, X. Hou, Q. Ru, H. Yu, L. Zhao, W. Li, *Chin. Sci. Bull.* **2009**, *54*, 1003.

[16] J.-H. Trill, C. Tao, M. Winter, S. Passerini, H. Eckert, *J. Solid State Electrochem.* **2011**, *15*, 349.

[17] a) Y. Oumellal, N. Delpuech, D. Mazouzi, N. Dupre, J. Gaubicher, P. Moreau, P. Soudan, B. Lestriez, D. Guyomard, *J. Mater. Chem.* **2011**, *21*, 6201; b) B. Key, M. Morcrette, J.-M. Tarascon, C. P. Grey, *J. Am. Chem. Soc.* **2011**, *133*, 503.

[18] W. Wei, F. Björefors, L. Nyholm, *Electrochim. Acta* **2015**, *176*, 1393.

[19] D. Rehnlund, C. Ihrfors, J. Maibach, L. Nyholm, *Mater. Today* **2018**, *21*, 1010.

[20] J. C. Li, N. J. Dudney, X. C. Xiao, Y. T. Cheng, C. D. Liang, M. W. Verbrugge, *Adv. Energy Mater.* **2015**, *5*.

[21] Z. H. Wang, M. K. Li, C. Q. Ruan, C. J. Liu, C. Zhang, C. Xu, K. Edström, M. Strömme, L. Nyholm, *J. Phys. Chem. C* **2018**, *122*, 23352.

[22] a) T. Pajkossy, *J. Electroanal. Chem. Interfacial Electrochem.* **1991**, *300*, 1; b) H. Olsson, M. Strömme, L. Nyholm, M. Sjödin, *J. Phys. Chem. C* **2014**, *118*, 29643.

[23] F. Lindgren, D. Rehnlund, I. Källquist, L. Nyholm, K. Edström, M. Hahlin, J. Maibach, *J. Phys. Chem. C* **2017**, *121*, 27303.

[24] F. Lindgren, C. Xu, L. Niedzicki, M. Marcinek, T. Gustafsson, F. Björefors, K. Edström, R. Younesi, *ACS Appl. Mater. Interfaces* **2016**, *8*, 15758.

[25] C. Xu, F. Lindgren, B. Philippe, M. Gorgoi, F. Björefors, K. Edström, T. Gustafsson, *Chem. Mater.* **2015**, *27*, 2591.

[26] M. Verbrugge, X. C. Xiao, Q. L. Zhang, M. Balogh, K. Raghunathan, D. Baker, *J. Electrochem. Soc.* **2017**, *164*, A156.